ELSEVIER

7 April 2000

Chemical Physics Letters 320 (2000) 339–344

CHEMICAL PHYSICS LETTERS

www.elsevier.nl/locate/cplett

# Spatial concentration and temperature distribution of CH radicals formed in a diamond thin-film hot-filament reactor

U. Lommatzsch [a], E.H. Wahl [b], T.G. Owano [b], C.H. Kruger [b], R.N. Zare [a,*]

[a] *Department of Chemistry, Stanford University, Stanford CA 94305-5080, USA*
[b] *Department of Mechanical Engineering, Stanford University, Stanford CA 94305, USA*

Received 22 February 2000

**Abstract**

Spatial concentration and temperature profiles of the CH radical in a hot-filament chemical vapor deposition reactor are measured by cavity ring-down spectroscopy. The CH concentration is found to be on the order of $10^{11}$ molecules/cm$^3$. The spatial distribution indicates that CH formation primarily occurs at or very near the filament. At a distance of 2 mm from the filament the $[H]/[H_2]$ ratio is determined to be $0.011 \pm 0.003$. © 2000 Elsevier Science B.V. All rights reserved.

## 1. Introduction

The outstanding physical and chemical properties of diamond thin films have led to a variety of applications in areas such as thermal management in microelectronic devices and coating materials for drilling tools [1,2]. Diamond films are usually synthesized by a chemical vapor deposition (CVD) process, e.g., in a hot-filament reactor (HF-CVD). The deposition of the diamond film on a substrate occurs via activation of molecular hydrogen and methane flowing over a hot wire. The activation includes the dissociation of hydrogen and the formation of various $C_xH_y$ species [3]. A complex series of gas-phase and surface reactions lead to diamond deposition. The major carbon species in the gas phase are linked by hydrogen-shift reactions

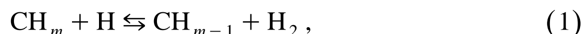

$$CH_m + H \leftrightharpoons CH_{m-1} + H_2\,, \tag{1}$$

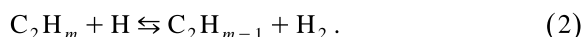

$$C_2H_m + H \leftrightharpoons C_2H_{m-1} + H_2\,. \tag{2}$$

Despite many efforts to achieve larger growth rates while maintaining quality in the film deposition process, growth rates are still limited to a few micrometers per hour. This growth rate prevents the use of diamond films in a large number of applications because of the high cost. A rational attempt to improve process performance requires a detailed understanding of all relevant steps in the CVD process.

This Letter focuses on the CH radical that has previously not been extensively studied owing to its low abundance in the HF-CVD reactor. Cavity ring-down spectroscopy (CRDS) is used to measure the gas-phase concentration and temperature of the CH radical. This new technique for absorption spec-

* Corresponding author. Fax: +1-650-723-9262; e-mail: zare@stanford.edu

0009-2614/00/$ - see front matter © 2000 Elsevier Science B.V. All rights reserved.
PII: S0009-2614(00)00250-5

troscopy is highly sensitive with detection limits that can be made to approach the shot-noise limit [4]. Moreover, CRDS allows for in-situ measurements with high spatial resolution [5,6]. In CRDS we record the decay rate of the intensity of a light pulse circulating in a high-finesse optical cavity formed by two highly reflective mirrors. In an empty cavity the intensity loss (decay rate) is mainly caused by losses of the mirrors. Filling the cavity with an absorbing substance leads to a faster decay rate because of additional losses caused by sample absorption. To good approximation, the intensity $I$ follows a single exponential decay with a characteristic time constant $\tau$ (see Eq. (3)), if the spectral width of the light pulse (laser linewidth) is larger than the free spectral range of the cavity and smaller than the width of the absorption features [7,8].

$$I(t) = I_0 \exp(-t/\tau) . \tag{3}$$

The absorbance $A$ of a sample is related to the number density $N$ of the absorbers by the absorption cross-section $\sigma$ and the path length $l$ (Beer–Lambert law). By measuring the ring-down time for the empty cavity and for the cavity filled with an absorber the absorbance is obtained (Eq. (4), where $t_r$ is the round-trip time and $\tau_0$ and $\tau$ are the ring-down time constants for an empty and a filled cavity, respectively). Therefore, no calibration is necessary and quantification is easily achieved.

$$A = \sigma \cdot N \cdot l = \frac{t_r}{\tau}\left(\frac{1}{\tau} - \frac{1}{\tau_0}\right) . \tag{4}$$

Using this technique, spatial concentration and temperature profiles of the CH radical in a hot-filament reactor are presented here.

## 2. Experimental

Only a brief description of the experimental setup (Fig. 1) is given here. Details can be found in Refs. [9,10]. The CVD reactor is maintained at a pressure of 20 Torr with a mixture of 1% $CH_4$ in $H_2$ flowing through the reactor at a flow rate of 100 sccm. The straight filament is made out of tungsten, 2 cm in length, and 200 μm in diameter. It is resistively heated. The substrate is a molybdenum strip resistively heated to ~ 1200 K and positioned parallel to the filament at a distance of 7 mm from it.

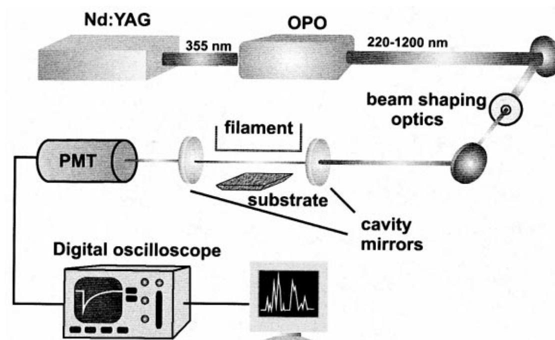


Fig. 1. Schematic of the experimental setup. A Nd:YAG laser pumped optical parametric oscillator OPO (Quanta-Ray PRO and MOPO-SL 710, Spectra Physics) with a repetition rate of 10 Hz and a bandwidth of $< 0.1$ $cm^{-1}$ is used as the light source. To match the light pulses to the $TEM_{00}$ mode of the optical cavity, a system of pinholes and lenses is used before introducing the light into the cavity. The filament can be rotated by 90°, which allows the light path to be either parallel or perpendicular to the filament axis.

The optical cavity is constructed from two plano-concave mirrors with a 6 m radius of curvature (Los Gatos Research), which are mounted to the reactor with a spacing of 65 cm. The intensity decay is monitored by a photomultiplier (EMI 9558QB) detecting the light leaking out of one of the cavity mirrors. The decay curve is digitized by a 8 bit, 1 GSample digital oscilloscope (HP 54510A) and the natural logarithm of each ring-down transient is fitted to a straight line on a PC. Typically, ring-down time constants of 30 individual decays are averaged for one data point. Only the part of the decay trace between 90% and 10% of the maximum intensity is used in the fitting process to avoid interference from noise and mode beating. The losses of the empty cavity are determined from the baseline of the Gaussian fitting procedure used to evaluate the peak intensities.

## 3. Results

The CH $A\,^2\Delta - X\,^2\Pi$ band system around 431 nm is probed for the concentration measurements. Fig. 2 presents a portion of the Q-branch members of the

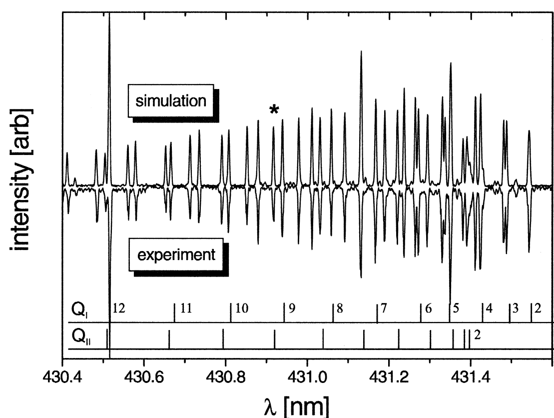


Fig. 2. Simulated (top) and experimental (bottom) Q-branch lines of the CH A-X (0,0) band. Transitions originating from the $^2\Pi_{3/2}$ and $^2\Pi_{1/2}$ states are labeled by $Q_I(N)$ and $Q_{II}(N)$, respectively. The simulation was made by using LIFBASE 1.5 [11] assuming a rotational temperature of 1400 K. The line marked with an asterisk was used for the concentration measurements owing to a minimum of interference with other lines.

CH absorption spectrum together with a simulated spectrum [11]. The splitting of the rovibronic levels by spin–orbit coupling and Λ-type doubling is clearly resolved, and the line positions are in excellent agreement with the literature [12,13]. For these transitions the Einstein coefficients have been determined previously [14]. The absorption cross-section for the concentration evaluation is calculated from these Einstein coefficients and the partition function at the respective gas temperature [15]. The gas temperature is determined from a Boltzmann plot, that typically included the Q-branch lines with the rotational quantum numbers $N'' = 5–15$. For the path length in Eq. (4) a value of 7.5 mm is used, which is significantly smaller than the filament length of 20 mm. This value was derived from a comparison with Abel inverted data from measurements with the filament placed perpendicular to the light path [10].

Fig. 3 shows the results from the temperature measurements, which illustrate the CH temperature as a function of distance from the filament and the dependence of gas temperature on the filament temperature at a fixed distance of 2 mm. With increasing distance from the filament a drop of temperature from 1500 to 1200 K is observed (Fig. 3a). Surprisingly, even at a distance of only 1.5 mm from the hot wire the gas-phase temperature is $\sim$ 1000 K below the filament temperature. Fig. 3b shows that an increase of filament temperature by 100 K induces an increase in gas temperature by 400 K. Therefore the temperature difference between filament and gas becomes somewhat smaller at higher filament temperatures.

Fig. 4 presents the CH concentration as a function of location and its dependence on filament temperature. As can be seen in Fig. 4a, the CH concentration, which is on the order of $10^{11}$ molecules/cm$^3$, decreases rapidly with increasing distance from the filament. Furthermore the concentration profile is symmetric on both sides of the filament (adjacent and distant to the substrate). The temperature dependence shows the onset of a strong increase of CH concentration when the filament temperature is above

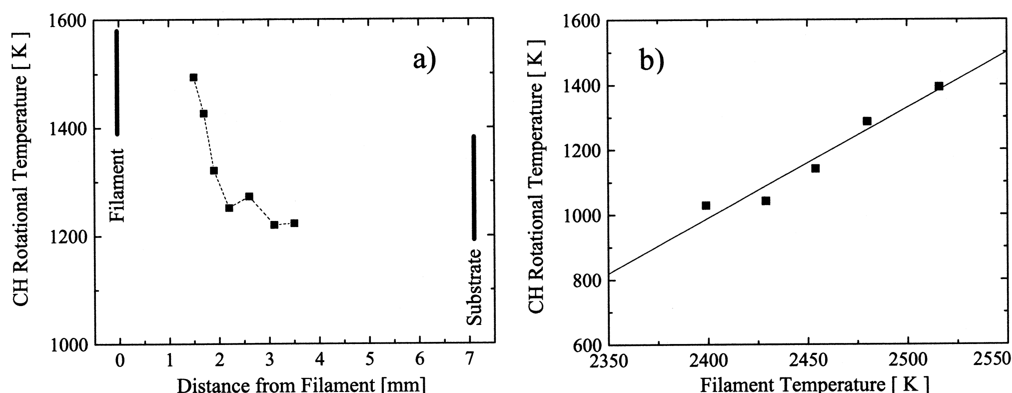


Fig. 3. Rotational temperature of CH ($v'' = 0$) as (a) a function of distance from the filament and (b) as a function of filament temperature at 2 mm distance from the filament. The filament temperature is 2500 K as measured by optical pyrometry.

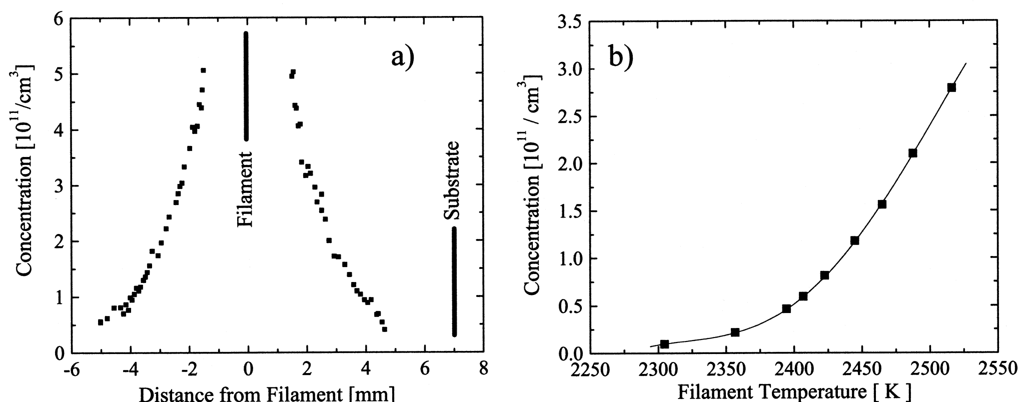


Fig. 4. CH concentration (a) at different filament distances at a filament temperature of 2500 K and (b) at different filament temperatures at a distance of 2 mm from the filament.

~ 2400 K (see Fig. 4b). No saturation in CH density with increasing temperature has been observed at the highest temperatures that we could achieve without destroying the filament.

The absolute uncertainty in the reported concentration values is 25%. This estimate is made by considering the uncertainties in the absorption cross-section (15%), the measurement of the ring-down time constant (1%) and the path length (20%) as the main contributions to the overall error. The error in the temperature measurements is estimated to be $\pm 100$ K (from the error statistics of the fit), which leads to an error of 15% in the calculation of the absorption cross-section from the tabulated Einstein coefficients [14].

## 4. Discussion

The CH radical in a CVD reactor under typical process conditions was studied comprehensively with CRDS as the diagnostic tool. Fig. 4a shows the maximum of the CH concentration very close to the filament. The CH temperature also has its maximum at this location (Fig. 3a). Both results suggest that the highest CH formation rate takes place at or near the filament. This conclusion is in striking contrast to results obtained for $CH_3$ in this laboratory, where a concentration maximum was found at a distance of 4 mm from the filament [9]. These data suggest large differences between both radicals in either the formation mechanism or their dependence on the $H/H_2$ ratio. The decrease of CH concentration with increasing filament distance can be crudely rationalized by taking geometrical dilution in the diffusion process and a decrease of H-atom density into account.

The typical CH concentration in the reactor is on the order of $10^{11}$ molecules/cm$^3$. The CH number densities differ only by a maximum factor of 3 from the CH concentrations measured by Childs et al. [16,17] in a hot-filament reactor with conventional absorption spectroscopy. This difference may be attributed to a much longer filament and other differences of the CVD reactor in the work of Childs et al. These concentrations are also similar to what has been reported by Stolk and ter Meulen [18] for a diamond depositing oxyacetylene flame. CH number densities on the order of $10^{10}$–$10^{12}$ molecules/cm$^3$ have been also found in methane/air flames by Derzy et al. [19] and in a plasma by Engeln et al. [20].

The $CH_3$ concentration in our reactor under nearly identical conditions was previously determined to be on the order of $10^{13}$ molecules/cm$^3$ [9,21]. The difference in CH and $CH_3$ number density by more than two orders of magnitude confirms the general view that CH is not one of the main species for diamond growth [3].

A comparison of our experimental CH concentration with values from theoretical simulations [22,23], which take only gas-phase chemistry into account, seems to indicate an underestimation of CH in the

simulations by a factor of 3–10. Based on differences in the reaction conditions between the experimental data and these models, this deviation is only estimated. Because the gas-phase chemistry is presumably well described by the theory, the discrepancy must be related to insufficient modeling of the heterogeneous reactions at the filament. This deviation indicates therefore an additional, heterogeneous, formation route for CH. The extent of this production process cannot be quantified from our results.

The hydrogen dissociation ratio $[H]/[H_2]$ is calculated from the measured CH and $CH_3$ number densities with a partial equilibrium analysis outlined by Childs et al. [17]. In this computation only the equilibrium constants [24] for the reactions (1) with $m = 0–4$ are used, assuming partial equilibrium between those hydrogen shift reactions. The hydrogen dissociation ratio is a crucial input for theoretical simulations. Performing this calculation for 1350 K yields a hydrogen dissociation ratio of $0.011 \pm 0.003$ at a distance of 2 mm from the filament. (The actual experimental data are taken from measurements with 0.5% input methane fraction to allow for the comparison with the methyl data.) This result is somewhat lower than the value of 0.022 derived by Childs et al. [17].

The symmetric concentration decay on both sides of the filament (Fig. 4a) indicates a negligible influence of substrate processes on the CH concentration. It also shows, that the flow of methane and hydrogen from the inlet into the reactor is more appropriately described as random molecular motion. This conclusion follows also from calculated Peclet numbers for very similar process conditions predicting diffusion as the dominant transportation mode [22]. Because concentration measurements closer to the substrate as shown in Fig. 4a were not possible (reaching the quantification limit), a substrate influence on CH distribution in the very vicinity of the substrate cannot be completely ruled out.

The temperature dependence of CH production is qualitatively similar to what Ashfold and co-workers [25] found for the hydrogen atom by REMPI measurements. For both species the production rate increases strongly when the filament temperature reaches $\sim 2400$ K. Because the hydrogen-atom production is related to a surface process at the filament, this temperature range appears to be the start of a high activity of the filament. Besides gas-phase production of CH, a heterogeneous process at the filament might therefore contribute to CH formation.

The large difference between the filament temperature and the gas temperature, shown in Fig. 3a, is remarkable. This temperature discontinuity was observed also in a variety of studies of hot-filament reactors [25–31]. It was explained by the breakdown of the (continuum) energy conduction theory at the low pressures in the reactor [32]. The time that molecules stick to the filament surface might not be long enough for thermal equilibration (equivalent to a small accommodation coefficient). As a consequence, molecules originating from the filament surface have a lower temperature than the filament.

## Acknowledgements

U.L. gratefully acknowledges support from the Deutsche Forschungsgemeinschaft. This work was supported by the Engineering Research Program of the Office of Basic Energy Sciences at the Department of Energy.

## References

[1] S.T. Lee, Z. Lin, X. Jiang, Mater. Sci. Eng. R 25 (1999) 123.
[2] M.N.R. Ashfold, P.W. May, C.A. Rego, N.M. Everitt, Chem. Soc. Rev. 23 (1994) 21.
[3] D.G. Goodwin, J.E. Butler, in: M.A. Prelas, G. Popovici, L.K. Bigelow (Eds.), Handbook of Industrial Diamonds and Diamond Films, Marcel Dekker, New York, 1998, p. 527.
[4] M.D. Levenson, B.A. Paldus, T.G. Spence, C.C. Harb, J.S. Harris, R.N. Zare, Chem. Phys. Lett. 290 (1998) 335.
[5] A. O'Keefe, D.A.G. Deacon, Rev. Sci. Instru. 59 (1988) 2544.
[6] K.W. Busch, M.A. Busch (Eds.), Cavity-Ringdown Spectroscopy, American Chemical Society, Washington, DC, 1999.
[7] J.T. Hodges, J.P. Looney, R.D. van Zee, Appl. Opt. 35 (1996) 4112.
[8] J. Martin, B.A. Paldus, P. Zalicki, E.H. Wahl, T.G. Owano, J.S. Harris, C.H. Kruger, R.N. Zare, Chem. Phys. Lett. 258 (1996) 63.
[9] P. Zalicki, Y. Ma, R.N. Zare, E.H. Wahl, T.G. Owano, C.H. Kruger, Appl. Phys. Lett. 67 (1995) 144.
[10] E.H. Wahl, T.G. Owano, C.H. Kruger, U. Lommatzsch, D. Aderhold, R.N. Zare, in: J.C. Angus, W.D. Brown, J.P. Dismukes, M.D. Drory, A. Gicquel, A. Grill, R.H. Hauge, H. Kawarada, C.P. Klages, R.L. Opila, A. Paoletti, Y. Sato, K.E. Spear, B.V. Spitsyn (Eds.), Diamond Materials VI,

Proc. Elelectrochem. Soc PV99-32, The Electrochemical Society, Pennington, 1999, in press.

[11] J. Luque, D.R. Crosley, LIFBASE: Database and Spectral Simulation Program (Version 1.5), SRI International Report MP 99-009, 1999.

[12] P.F. Bernath, C.R. Brazier, T. Olsen, R. Hailey, W. Fernando, C. Woods, J.L. Hardwick, J. Mol. Spectrosc. 147 (1991) 16.

[13] M. Zachwieja, J. Mol. Spectrosc. 170 (1995) 285.

[14] J. Luque, D.R. Crosley, J. Chem. Phys. 104 (1996) 2146.

[15] G.A. Bethardy, R.G. Macdonald, J. Chem. Phys. 103 (1995) 2863.

[16] M.A. Childs, K.L. Menningen, H. Toyoda, L.W. Anderson, J.E. Lawler, Europhys. Lett. 25 (1994) 729.

[17] M.A. Childs, K.L. Menningen, H. Toyoda, Y. Ueda, L.W. Anderson, J.E. Lawler, Phys. Lett. A 194 (1994) 119.

[18] R.L. Stolk, J.J. ter Meulen, Diam. Relat. Mater. 8 (1999) 1251.

[19] I. Derzy, V.A. Lozovsky, S. Cheskis, Chem. Phys. Lett. 306 (1999) 319.

[20] R. Engeln, K.G.Y. Letourneur, M.G.H. Boogaarts, M.C.M. van de Sanden, D.C. Schram, Chem. Phys. Lett. 310 (1999) 405.

[21] P. Zalicki, Y. Ma, R.N. Zare, E.H. Wahl, J.R. Dadamio, T.G. Owano, C.H. Kruger, Chem. Phys. Lett. 234 (1995) 269.

[22] D.G. Goodwin, G.G. Gavillet, J. Appl. Phys. 68 (1990) 6393.

[23] D.S. Dandy, M.E. Coltrin, J. Appl. Phys. 76 (1994) 3102.

[24] R.J. Kee, F.M. Rupley, J.A. Miller, Sandia National Laboratories Reports SAND-8215B and SAND89-8009B, CHEMKIN, 1992.

[25] S.A. Redman, C. Chung, K.N. Rosser, M.N.R. Ashfold, Phys. Chem. Chem. Phys. 1 (1999) 1415.

[26] C. Kuei-Hsien, C. Mei-Chen, C.M. Penney, W.F. Banholzer, J. Appl. Phys. 71 (1992) 1485.

[27] S.J. Harris, A.M. Weiner, T.A. Perry, Appl. Phys. Lett. 53 (1988) 1605.

[28] L.L. Connell, J.W. Fleming, H.N. Chu, D.J. Vestyck Jr., E. Jensen, J.E. Butler, J. Appl. Phys. 78 (1995) 3622.

[29] K.L. Menningen, M.A. Childs, L.W. Anderson, J.E. Lawler, Rev. Sci. Instrum. 67 (1996) 1546.

[30] G. Leyendecker, J. Doppelbauer, D. Baeuerle, P. Geittner, H. Lydtin, Appl. Phys. A 30 (1982) 237.

[31] V. Zumbach, J. Schaefer, J. Tobai, M. Ridder, T. Dreier, T. Schaich, J. Wolfrum, B. Ruf, F. Behrendt, O. Deutschman, J. Warnatz, J. Chem. Phys. 107 (1997) 5918.

[32] I. Langmuir, J. Am. Chem. Soc. 37 (1915) 417.